ECS Transactions, 3 (31) 531-544 (2007)
10.1149/1.2789255, copyright The Electrochemical Society

Use of Coupled Electrode Arrays to Elucidate Copper Pitting as a Function of Potable Water Chemistry

H. Cong[a], N. D. Budiansky[a], H. T. Michels[b] and J. R. Scully[a]

[a]Center for Electrochemical Science and Engineering, Department of Materials Science and Engineering, University of Virginia, Charlottesville, Virginia 22904, USA
[b]Copper Development Association Inc., 260 Madison Ave., New York, New York 10016, USA

The electrochemical pitting behavior of UNS C11000 copper was investigated in synthetic potable water and several other HCO_3^-, SO_4^{2-} and Cl^- containing waters using microelectrodes and coupled multi-electrode arrays. Studies were systematically conducted (pH from 6 to 10, $[Cl_2]$ (as NaOCl) from 1-5 ppm, and with or without $Al(OH)_3$ additions). Studies of the effect of water chemistry on electrochemical properties of copper were accomplished using the cyclic voltammetry and cathodic polarization methods. Critical potentials for copper pitting are observed to be brought about and decreased by certain water chemistry variables. High $[SO_4^{2-}]/[HCO_3^-]$ and $[Cl^-]/[HCO_3^-]$ lower pitting potentials (E_{Pit}) while high $[HCO_3^-]$ and pH raise E_{Pit}. ClO^- increases cathodic reaction rates and thus raises OCPs towards E_{Pit}. Certain water chemistries (pH from 8 to 10, $[Cl_2] > 2$ ppm and with $Al(OH)_3$) are found to promote pitting conditions where strong, persistent anodes developed at certain sites and pitting factor was raised.

Introduction

Copper tubes account for more than 80% of all tubes in potable water systems in buildings in the U.S.A. Among all the failures of copper piping that occur, "pinhole" pitting corrosion accounts for more than 60% (1). Failures by pinhole pitting occur in certain potable waters but not others. Pitting corrosion can lead to premature failure of copper tube due to rapid penetration of the tube wall in local areas.

Regardless of details regarding the exact water chemistry, one consistent aspect is that there is a critical potential associated with pitting. That is, if the open circuit potential rises above a critical pitting potential value, which depends on the materials and the environment, pitting corrosion occurs. This phenomenon can occur under specific water chemistries (2-4) or material conditions (1). For instance, Edwards and Marshall demonstrated that a synergistic reaction between free residual chlorine (5 ppm Cl_2) and aluminum solids (2 ppm Al-$Al(OH)_3$) created particularly aggressive conditions for copper pipe pitting in high pH (pH = 9) potable water, based on a synthetic water recipe from Washington Suburban Sanitary Commission (WSSC). These findings were duplicated in lab exposures (5,6). However, a scientific understanding of roles of free chlorine and aluminum solids on cold water copper piping is currently lacking (5). Moreover, such pitting is hard to reproduce in laboratory experiments even when water chemistries are replicated.

Downloaded on 2016-09-15 to IP 130.203.136.75 address. Redistribution subject to ECS terms of use (see ecsdl.org/site/terms_use) unless CC License in place (see abstract).

SO_4^{2-}, HCO_3^- and Cl^- are three important anions in potable water. The effect of each ion on the stability of the passive film on copper has been widely studied in different environments. Milosev et al., studied the aggressive nature of SO_4^{2-} and inhibiting nature of HCO_3^-, and developed a quantitative relationship between breakdown potential and $[SO_4^{2-}]$ and $[HCO_3^-]$ at pH = 8.3 (7). Mattsson et al., did their research on $[HCO_3^-]/[SO_4^{2-}]$ ratio based on a potable water concentration, and determined that a critical ratio must be achieved to prevent hard copper from pitting corrosion (8). Drogowka et al., found $[Cl^-]$ promotes the breakdown of passive film and shifts the breakdown potential towards more negative value at pH = 8. The HCO_3^- ions have an inhibiting influence against the aggressive attack of Cl^- (9). Duthil suggested that in the presence of both SO_4^{2-} and Cl^-, the competition of the two ions makes the pitting behavior of Cu more complex than with only one type of anions (10). In summary, it is generally agreed that SO_4^{2-} and Cl^- promote the breakdown of passive film, and HCO_3^- is effective in counteracting and promoting passivity. SO_4^{2-} ions are generally more aggressive than Cl^- (10). Given this understand of anions, the role of Cl_2 can be speculatively related to creating a high OCP near E_{Pit} as influenced by these water chemistry variables. The exact role of aluminum solids remains unclear.

The focus of this research on the pitting of copper is aimed at establishing the connection between specific water chemistries identified to cause cold water pitting (5,6) and the salient electrochemical conditions that enable such pitting. Systematic variations are made in the chemistry of the synthetic water recipe used by Edwards (5,6) with the aim of determining the role in altering the electrochemical factors that govern pitting susceptibility. Comparisons are made between the electrochemical properties of Cu in waters that do not cause pitting and those that do. The outcome will be a better understanding of how certain water chemistries bring about the specific electrochemical conditions that enable cold water pitting.

Experimental Procedures

A conventional three electrode electrochemical cell was used. The working electrodes were constructed from different diameter (150 and 250 μm) high purity grade UNS C11000 copper wires (>99.9%). The wires were embedded in epoxy resin and cast in mounting molds and carefully polished using successively finer SiC abrasive papers (600-800-1200 grit) lubricated with water, degreased in acetone, rinsed in deionized water, and dried at room temperature. The counter electrode was a platinum-niobium mesh. Potentials were measured by a Hg/Hg_2SO_4 reference electrode in cyclic voltammetry experiments and by a saturated calomel electrode in cathodic polarization and multi-electrode array experiments. For convenience, all the potentials were quoted versus a saturated calomel electrode (SCE).

Environments

In cyclic voltammetry tests, test solutions to study the effect of different anions (Cl^-, HCO_3^-/CO_3^{2-}, SO_4^{2-}) were prepared by adding various mixtures of analytical grade reagents, NaCl, $NaHCO_3$, and Na_2SO_4 in deionized water. TABLE 1 and TABLE 2 list all the combinations of ions that have been used to develop the pitting stability domains of HCO_3^-—Cl^- and HCO_3^-—SO_4^{2-} at pH =8.3 and pH = 9.5.

Downloaded on 2016-09-15 to IP 130.203.136.75 address. Redistribution subject to ECS terms of use (see ecsdl.org/site/terms_use) unless CC License in place (see abstract).

TABLE 1. Cyclic voltammetry test matrix for exploring HCO_3^-—SO_4^{2-} chemistry (pH = 8.3 and 9.5)

	$[HCO_3^-]$ (M)			
	34 mg/L*	**0.001**	**0.01**	**0.1**
$[SO_4^{2-}]$ (M)	14 mg/L*	0.0005	0.005	0.1
	24 mg/L*	0.001	0.01	0.3
	34 mg/L*	0.003	0.03	0.5
	68 mg/L*	0.005	0.05	1

** Based on synthetic water composition, unit of mg/L is used instead of M.*

TABLE 2. Cyclic voltammetry test matrix for exploring HCO_3^-—Cl^- chemistry (pH = 8.3 and 9.5)

	$[HCO_3^-]$ (M)			
	34 mg/L*	**0.001**	**0.01**	**0.1**
$[Cl^-]$ (M)	20 mg/L*	0.0005	0.005	0.05
	30 mg/L*	0.001	0.01	0.1
	40 mg/L*	0.003	0.03	0.5
	80 mg/L*	0.005	0.05	1
		0.01	0.1	3
			0.3 **	
			0.5 **	
			1 **	

** Based on synthetic water composition, unit of mg/L is used instead of M.*
*** Experiments only performed at pH = 9.5, not pH = 8.3*

The synthetic water used in this research was designed to simulate the gross ionic constituents of WSSC water (6). The water initially contained 34 mg/L alkalinity as HCO_3^-, 14 mg/L SO_4^{2-}, 20 mg/L Cl^-, and 17 mg/L Ca^{2+} added as reagent grade sodium or calcium salts to deionized water, which has a conductivity of 148 μS/cm. Chlorine residue was added in the form of purified grade sodium hypochlorite (4-6% NaOCl), and free chlorine was measured by using the DPD colorimetric test per standard method 4500-Cl G (5,6). At high pH, ClO^- is the dominant species of chlorine, and at pH below 7.5, HClO is the major form. Cl_2 is only significant at pH < 5 (11,12). The conversion from ClO^- to HClO has an influence on the electrochemical factors controlling pitting of copper, as demonstrated in cathodic polarization experiments and multi-electrode array experiments. The stock solution for $Al(OH)_3$ solids was created by raising the pH of 3000 mg/L $AlCl_3$ solution to pH = 8.0 using NaOH, followed by repeated washing with reagent grade water (followed by solid settling) until the conductivity of the solution was equal to or less than the experimental water.

In all the test solutions, pH was adjusted to designated value by adding droplets of either 1M NaOH or 1M HCl. Deaeration was achieved by bubbling high purity nitrogen gas through test solutions for at least two hours, which was true for all the cyclic voltammetry tests and some of the cathodic polarization experiments.

Cyclic Voltammetry Experiments. The cyclic voltammetry technique has been used to study the electrochemical characteristics associated with copper oxidation, film and scale development as well as copper pitting. All cyclic voltammetry and cathodic polarization

Downloaded on 2016-09-15 to IP 130.203.136.75 address. Redistribution subject to ECS terms of use (see ecsdl.org/site/terms_use) unless CC License in place (see abstract).

experiments were performed using the same FAS2^{TM} Femostat by Gamry, which is ideally suited for making measurements on microelectrodes. A Faraday cage was used to eliminate electrical noise. All the experiments were performed at room temperature, 25ºC. A 250 µm diameter wire was mainly used for cyclic voltammetry experiments. Prior to testing, a cathodic potential of -0.6 V was applied to the working electrode for 10 minutes to remove any trace of air-formed oxide on the metal surface. Cyclic voltammetry scans started at -0.6 V, scanned up to +0.3 V in the anodic direction, and back to -0.8 V in the cathodic direction at the scan rate of 1 mV/sec. Three cycles were scanned in one experiment via continuous cycling for -0.8 V to +0.3 V to achieve repeatable results. After the experiments, the electrode surface was examined by an optical microscope to study the pitting morphology and exclude experiments corrupted by crevice corrosion.

Cathodic Polarization Experiments. A 150 µm copper working electrode was mainly used, and the test solutions were synthetic water. The working electrode was held at open circuit potential for 90 minutes, after which, it was cathodically polarized to -1.5 V at the scan rate of 2 mV/sec. Experiments have been repeated to test the reproducibility of results.

Multi-electrode Array (MEA) Experiments. Close packed arrays of copper electrodes, which are ideally suited for study of persistent anodes and cathodes, were utilized (13). Since localized pitting phenomena require separation of anodes and cathodes, fast anodic reaction rates on local areas and the formation of high cathode/anode area ratios can be detected as a function of water chemistry if electrodes are on the size scale of anodes. 5x20 multi-electrode arrays were constructed from 150 µm diameter copper wires with a nominal separation distance of 30 µm, with a total area of equivalent rectangle of 2.25 mm^2 (3 mm x 0.75 mm) as shown in FIGURE 1. Arrays were flush mounted in epoxy resin to simulate a planar copper electrode surface and polished with successively fine abrasive paper (600-800-1200 grit) to the desired finish. A Model 900 Multichannel Microelectrode Analyzer (MMA) (Scribner Associates, Inc.) was used for multi-electrode array experiments (13).

In the MEA experiments, free chlorine was adjusted incrementally every 24 hours from 0 ppm to 5 ppm. The target level of chlorine was increased as follows: 0, 1, 2, 3, 4, 5 ppm as Cl_2. Targeted pH values of 6, 7, 8, 9 and 10 were tested. Water was changed every 24 hours and no intent was made to maintain the pH and chlorine concentration during the 24 hours. The combined impacts of $Al(OH)_3$ and Cl_2 were examined by repeating the above tests, but with the addition of 2 ppm $Al(OH)_3$ solids.

Result

Cyclic Voltammetry to Assess Passivity and Pitting

Synthetic Water Based Experiments. Copper cyclic voltammetry was performed in different pH synthetic water solutions with pH values of 5, 6, 7, 8.5, 9.5, 10 to 11. Based on the experiment results, as the pH decreases, the copper surface remains passivated until the pH is decreased below 8.5 as shown in FIGURE 2.

Effect of $H_2CO_3/HCO_3^-/ CO_3^{2-}$. Two sets of experiments were performed to study the effect of bicarbonate/carbonate ions versus pH: (a) $[CO_3^{2-}] + [HCO_3^-] = 0.01$ M,

Downloaded on 2016-09-15 to IP 130.203.136.75 address. Redistribution subject to ECS terms of use (see ecsdl.org/site/terms_use) unless CC License in place (see abstract).

adjusting pH from 5, 6, 7, 8.5 to 9.5 (FIGURE 3), (b) $[CO_3^{2-}]$ + $[HCO_3^-]$ = 0.1 M, adjusting pH from 5, 6, 7, 8.5 to 9.5. As shown in FIGURE 3, in the presence of 0.01 M HCO_3^-, the copper electrode surface remains passive until pH is decreased below 7. By comparison, in the presence of 0.1 M HCO_3^-, passivation is maintained until the pH is decreased below 6. As a result, higher concentration of HCO_3^- can be added in order to improve the passivation of copper in lower pH environments. When passivation is rendered less stable at low pHs (FIGURE 3), only the anodic direction of the cyclic voltammetry is shown in the figures, which is true throughout the entire section.

HCO_3^-—Cl^-, HCO_3^-—SO_4^{2-} Stability Domains. Stability domains of HCO_3^-—Cl^- and HCO_3^-—SO_4^{2-} against stable pitting have been developed at pH = 8.3 and pH = 9.5. The stability domains are developed in the following way: At pH = 8.3, a certain concentration of HCO_3^-, for example, 0.01 M, was added to different concentration of SO_4^{2-} solutions, which varied from 0.005, 0.01, 0.03, 0.05 to 0.1 M. As shown in FIGURE 4, when $[SO_4^{2-}] \leq 0.01$ M, the copper surface remained passive without pitting, and when $[SO_4^{2-}] > 0.01$ M, pitting occurred at high anodic potentials. The onset of pitting stabilization was characterized by dramatic increasing of current density as pits stabilize, usually ten times or greater, when the potential change was finite. The pitting potential defined in this way depended on $[SO_4^{2-}]$ in this example: High SO_4^{2-} levels caused the pitting potential to drop to between +0.1 V and +0.3 V. As the $[SO_4^{2-}]$ increased, the pitting potential decreased. However, no pitting potential has been seen at potential lower than -0.1 V, which corresponds to the reaction $2Cu + H_2O = Cu_2O + 2H^+ + 2e^-$.

The CO_3^{2-}—Cl^- pitting stability domain was developed in the same manner. An example is shown in FIGURE 5 at pH = 9.5 and with $[HCO_3^-]$ = 0.001 M. As the $[Cl^-]$ increased, the pitting potential decreased. However, no pitting potential was observed at potentials lower than -0.1 V, which corresponds to the reaction $2Cu + H_2O = Cu_2O + 2H^+ + 2e^-$.

FIGURE 6 - FIGURE 9 summarize the four stability domains that have been developed by determining the critical potential associated with pitting in each water chemistry. The star on each figure shows the basic concentration of synthetic water. Stability domains results show that higher $[Cl^-]/[HCO_3^-]$ or $[SO_4^{2-}]/[HCO_3^-]$ ratios lead to the local breakdown of passive film (pitting potential decreases with increasing $[Cl^-]$ or $[SO_4^{2-}]$) at a given pH. Meanwhile higher levels of $[HCO_3^-]$ create resistance to pit stability of passivited Cu at both pH = 8.3 and pH = 9.5. However, at pH = 8.3, low levels of $[HCO_3^-]$ (e.g., 0.001M) could even allow pitting at high applied potentials without Cl^- or SO_4^{2-}.

TABLE 3 lists the critical ion ratio that enabled pitting derived from the stability domain diagrams. FIGURE 10 is the corresponding figure. As shown in FIGURE 10, a small change of pH (from 8.3 to 9.5) has great influence on the critical ratio of $[Cl^-]/[HCO_3^-]$, while by comparison, pH has almost no influence on the critical ratio of $[SO_4^{2-}]/[HCO_3^-]$ indicating the aggressiveness of $[SO_4^{2-}]$. Moreover only limited protection was observed at $[HCO_3^-] < 0.001$ M at pH = 9.5. At pH = 8.3, Cl^- and SO_4^{2-} have almost the same effect on copper pitting as given by the standard of critical ion ratio, while at pH = 9.5, SO_4^{2-} is much more aggressive than Cl^- (i.e., the critical ion ratio of

Downloaded on 2016-09-15 to IP 130.203.136.75 address. Redistribution subject to ECS terms of use (see ecsdl.org/site/terms_use) unless CC License in place (see abstract).

$[SO_4^{2-}]/[HCO_3^-]$ is much lower than $[Cl^-]/[HCO_3^-]$). It should be noted that synthetic water would not be capable of lowering pitting potential to the natural OCP without the presence of something which shifts the $[SO_4^{2-}]/[HCO_3^-]$ ratio towards conditions more conducive to pitting.

TABLE 3. Critical ion ratio above which causes copper pitting as determined from cyclic voltammetry

$[HCO_3^-]$ (M)	pH = 9.5		pH = 8.3	
	$[SO_4^{2-}]/[HCO_3^-]$	$[Cl^-]/[HCO_3^-]$	$[SO_4^{2-}]/[HCO_3^-]$	$[Cl^-]/[HCO_3^-]$
$5.6x10^{-4}$ (34 mg/L)	0.4485	1.5	0.3*	1*
0.001	1	3	0**	0**
0.01	3	30	3	3
0.1	14***	30	14***	10

** These experiments were based on basic synthetic water, which had 34 mg/L HCO_3^-, 20 mg/L Cl^-, and 14 mg/L SO_4^{2-}, hence $[SO_4^{2-}]$ and $[Cl^-]$ had to be higher than the basic concentration.*
*** At pH = 8.3, cyclic voltammetry shows 0.001 M HCO_3^- could cause pitting at high potential, which is reproducible.*
**** At $[HCO_3^-]$ = 0.1 M, 1 M SO_4^{2-} didn't cause pitting either at pH = 9.5 or pH =8.3. Since the solubility of Na_2SO_4 at room temperature is about 1.4 M, 14 is used here. However, it doesn't necessarily mean that pitting would occur at this ratio.*

Potentiodynamic Scans to Elucidate Cathodic Half Cell Kinetics

The effect of free chlorine reduction was studied by varying the free chlorine concentration from 1 ppm to 5 ppm, at different pHs from 5 to 9.5. The results are shown in FIGURE 11 (pH = 9.5). Additionally, the effect of Al solids on the cathodic process in the synthetic water was studied. 2 ppm Al-$Al(OH)_3$ was added in the 5 ppm free Cl_2 synthetic water, and the pH was varied from 5 to 9.5. For comparison, 5 ppm Cl_2 synthetic water without Al-$Al(OH)_3$ was prepared, and pH was also varied from 5 to 9.5. FIGURE 12 shows an example of two polarization curves. All the conditions were the same (pH =9.5, 5 ppm Cl_2) except one synthetic water had 2 ppm Al-$Al(OH)_3$, while the other didn't. Currents extracted from polarization curves at the potentials of -0.1 V and -0.2 V at different pHs from 5 to 9.5 were plotted in FIGURE 13. No significant effect of $Al(OH)_3$ is observed on cathodic kinetics.

Chlorine reduction is the dominant cathodic reaction at the potential range near the pitting potential, and cathodic current is proportional to chlorine concentration at pH = 9.5, as shown in FIGURE 11. At pH = 8.5, the cathodic current doesn't depend in any systematic way on the free chlorine concentration, which might be attributed to the change of species from ClO^- to HClO (12). Al-$Al(OH)_3$ doesn't seem to affect the cathodic polarization process at high chlorine concentration (5 ppm) as shown in FIGURE 12 and FIGURE 13.

Multi-electrode Array (MEA) Experiment to Detect Persistent Anodes

FIGURE 14 (c) and (d) show the real time current maps which monitor currents of every single coupled wire in the MEA. Each square represents one corresponding single wire. A plus sign with a red background means the wire is acting as an anode, while a

Downloaded on 2016-09-15 to IP 130.203.136.75 address. Redistribution subject to ECS terms of use (see ecsdl.org/site/terms_use) unless CC License in place (see abstract).

minus sign with blue background represents a cathode. Dark blue represents a strong cathode and dark red corresponds to a strong anode.

As shown in FIGURE 14 (a), after the OCP rose to a critical level, which was about +100 mV, it suddenly dropped to a very low level in very short time. The current maps corresponding to these two times (denoted on OCP figure) showed that before the OCP reached critical level, only uniform passive dissolution of copper occurred. However, when the OCP dropped to about +40 mV, a dark square in the current maps indicated a current density about 70 $\mu A/cm^2$ averaged over the entire wire (if the pit area was only $1/10^{th}$ of wire surface, the current density was 700 $\mu A/cm^2$ or approximately 350 mpy). The high current density confirmed that a strong anode was forming. The current versus time curve for the strong anode wire during this period is shown in FIGURE 15. This represents net anodic current on this wire from the zero resistance ammeter (ZRA). Corresponding to the potential drop of OCP, an abrupt increase of current density occurred from less than 5 $\mu A/cm^2$ (uniform attack) to about 70 $\mu A/cm^2$ (localized attack). This strong anode lasted to the end of the experiment (12 hours), although the magnitude decreased over time. We interpret this result as evidence that a persistent anode was forming on one single wire in this water chemistry.

FIGURE 16 shows the OCP and local current behavior when 1, 3 and 4 ppm Cl_2 were added in pH = 9 synthetic water with the presence of 2 ppm Al-$Al(OH)_3$ on day 2, 4 and 5. The OCP gradually increased above the critical level as the chlorine concentration increased and pitting events signaled by current spikes appeared. A summary of the number of pitting events during the test is shown in TABLE 4, with a threshold current density of 40 $\mu A/cm^2$.

TABLE 4. Total number of distinct pitting events that occurred on all wires during MEA experiments over a 24 hour period.

$[Cl_2]$ (ppm)	**2 ppm Al-$Al(OH)_3$ pH**					**No Al-$Al(OH)_3$ pH**				
	6	**7**	**8**	**9**	**10**	**6**	**7**	**8**	**9**	**10**
5	6	4	***9***	***11***	5	0	2	2	4	1
4	5	2	***7***	***26***	2	9	1	4	4	2
3	4	***13***	***24***	***83***	1	0	0	***19***	4	1
2	1	***10***	***19***	0	0	4	2	***21***	7	0
1	0	2	0	0	0	0	0	0	0	0
0	0	0	0	0	0	0	0	0	0	0

* *Critical current limit: $7x10^{-9}$ A, ~ 40 $\mu A/cm^2$*

Discussion

Passivity and Pitting of Copper

Electrochemical kinetics studies substantiate the view that Cu is passivated with increasing pH and also with increasing HCO_3^- content in synthetic potable water. Evidence for this is the observation of Cu^0/Cu^+ and Cu^+/Cu^{++} oxidation peaks with reduction in dissolution rate after oxide formation as pH is increased and as HCO_3^- concentration is increased (FIGURE 2, FIGURE 3). Moreover, the Cu^{++}/Cu^+ and Cu^+/Cu^0

Downloaded on 2016-09-15 to IP 130.203.136.75 address. Redistribution subject to ECS terms of use (see ecsdl.org/site/terms_use) unless CC License in place (see abstract).

reduction peaks are seen at high pH. Coulometric determination of oxide thickness on Cu is a well-known procedure. In contrast, at pH less than 8.5 not only are reduction peaks not observed but the current near the Cu^+/Cu^{++} oxidation potential increases with small changes in potential (FIGURE 2). These findings are consistent with the E-pH thermodynamic behavior of the Cu-H_2O-25°C system which indicates Cu^{++} stability at low pH and Cu_2O as well as CuO stability at high pH levels. Moreover, the Cu-Cl-H_2O-CO_2-SO_3-25°C systems indicates $CuCO_3Cu(OH)_2$ stability at increasing pH and possibly $CuCO_3$. HCO_3^- improves passivity in CV by increasing the charge associated with the reduction peaks suggesting that a greater fraction of anodic charge could be attributed to oxide formation. It is interesting to note that pitting requires passive film formation and E_{Pit} was never reduced below the Cu^0/Cu^+ anode peak suggesting that pitting was not possible in low pH solutions.

Critical potentials for copper pitting are observed to be brought about and decreased by certain water chemistry variables. High $[SO_4^{2-}]/[HCO_3^-]$ and $[Cl^-]/[HCO_3^-]$ lower pitting potentials while high $[HCO_3^-]$ and high pH improve passivity and raise pitting potentials. It is interesting to note that the methodology of comparing E_{Pit} to E_{OCP} as frequently conducted for stainless steels(14) can be conducted for copper. At this critical threshold potential, local passive film breakdown and stabilization of pitting occur. This notion is substantiated by MEA studies which show abrupt E_{OCP} drops coincident with current spikes indicative of strong anode formation. Therefore, pitting of copper involves discrete, abrupt passive film breakdown events and is not explained by simple galvanic cells such as a differential aeration cell which would not likely indicate such current transients. Certain water chemistries promote a decrease in E_{Pit}. A rise in E_{OCP} brought about by chlorination can induce pitting if the waters are alkaline enough to promote passivity and if the anion mix drops E_{Pit} to E_{OCP}. It also stands to reason that anything else that raises E_{OCP} to E_{Pit} such as a carbon based films(15) can cause pitting in a water of the appropriate mix of anions. It is clear that E_{Pit} must be lowered towards +100 mV which is closed to the E_{OCP} obtained in highly chlorinated water.

It is interesting to note that the anion mix in synthetic water recipe used here would not lower E_{Pit} in the tests conducted here to potentials as low as +100 mV. In fact, the stars on FIGURE 6-FIGURE 9 indicate applied potential - anion concentration combinations that produce pit stabilization (i.e. E_{Pit}). These E_{Pit} values are far more positive than attainable E_{OCP} values at 5 ppm Cl_2. This raises an obvious question as to how pitting could be observed in such waters in service were polarization is restricted to the OCP. Speculatively, occluded cells created by $Al(OH)_3$ and other deposits may alter the anion ratios towards conditions more favorable for pitting. For instance, $Al(OH)_3$ might form an occluded site but act as a selective ion membrane. Other mechanisms exist as well such as chemical reactivity of specific deposits such as buffering and/or complexation or sequestering of selected species. Further studies will be required to elucidate the exact role of aluminum solids.

The coupled multi-electrode arrays provided information on formation of strong persistent anodes above and beyond what is possible with single working electrode experiments. While measurement of abrupt E_{OCP} drops or "noise" as indicated in FIGURE 16 provides evidence of pit events as Cl_2 is increased and does not require an MEA, the combination of E_{OCP} and local net currents from individual and persistent anodes provides substantially more information regarding the degree of persistent anode

Downloaded on 2016-09-15 to IP 130.203.136.75 address. Redistribution subject to ECS terms of use (see ecsdl.org/site/terms_use) unless CC License in place (see abstract).

development. It is possible to extract a pitting factor from MEA data as will be shown later. The combination of water chemistry conditions and array information such as number of pit events at a single electrode (e.g., at the same or nearby pit site) amongst many and the maximum anodic charge associated with a single site on a simulated planar electrode provides a level of information not obtained with single electrode measurements.

Technological Ramifications

The results of this study show that certain combinations of water chemistry, pH and chlorination bring about pitting of copper. Studies of corrosion propagation might further indicate damaging water chemistries in this stage of pitting. Assuming that these results hold for longer term exposures under flow, they can provide rapid assessment of presence of pitting waters and provide information to utilities concerning the danger of cold water pitting.

It is interesting to note that UNS C11000 duplicates all the results observed in the Edwards study (5,6) without the use of any specific copper piping. These results could be duplicated on different lots of copper tubing but so far do not indicate a metallurgical culprit that is related to a particular heat of copper tubing.

It is clear that changes in water chemistry, when made for any reasons by the provider, can result in unintended pitting attack and leaks in copper plumbing tube. In addition, the release of particulates also has the potential to contribute to pitting, because local chemistry is altered under the particles when they come to rest as deposits. It would be prudent for the providers of potable water to evaluate the potential impact of water treatment changes on the corrosion resistance of all components in a water system, from the source, through the distribution system and to the point of end use when consumed, prior to making any alterations in water chemistry. The MEA may prove useful in such an evaluation.

Conclusions

- The micro-electrode technique enables accurate electrochemical testing of copper in low conductivity solutions (e.g., synthetic drinking water).
- Cathodic polarization studies confirm that chlorine reduction is the dominant cathodic reaction when water is chlorinated. Aluminum solids don't increase the charge transfer or mass transport controlled cathodic reduction current from pH = 5 to pH = 9.5. However, the presence of aluminum solids could serve as occluded site and/or ion selective membrane that affects the anodic process.
- High $[SO_4^{2-}]/[HCO_3^-]$ and $[Cl^-]/[HCO_3^-]$ decreased the pitting potential at both pH = 8.3 and pH = 9.5. High $[HCO_3^-]$ and high pH promoted passivity of copper.
- The MEA was successful in detecting formation of persistent anodes compared to switchable anodes. More severe pit initiations occurred at high pH and high chlorine level. The presence of aluminum solids exacerbated copper pitting by an unknown mechanism.

Downloaded on 2016-09-15 to IP 130.203.136.75 address. Redistribution subject to ECS terms of use (see ecsdl.org/site/terms_use) unless CC License in place (see abstract).

Acknowledgements

Financial support from the Copper Development Association, Inc. under the direction of Dr. Harold Michels and Mr. Andy Krieta Jr. is gratefully acknowledged. The insightful advice of Professor Marc Edwards at Virginia Polytechnic Institute and State University is also gratefully acknowledged.

References

1. P.J.L. Fernandes, *Eng. Fail. Anal.*, **5**, 35 (1998).
2. Y. Feng, W.-K. Teo, K.-S. Siow, K.-l. Tan, and A.-K. Hsieh, *Corros. Sci.*, **38**, 369 (1996).
3. T. Fujii, T. Kodama, and H. Baba, *Corros. Sci.*, **24**, 901 (1984).
4. M. Edwards, J.F. Ferguson, and S.H. Reiber, *J. AWWA*, **86**, 74 (1994).
5. J.C. Rushing, and M. Edwards, *Corros. Sci.*, **46**, 3069 (2004).
6. B.J. Marshall, *Initiation, propagation, and mitigation of aluminum and chlorine induced pitting corrosion*, Master of Science, Virginia Polytechnic Institute and State University, Blacksburg, (2004).
7. I. Milosev, M. Metikos-Hukovic, M. Drogowska, H. Menard, and L. Brossard, *J. Electrochem. Soc.*, **139**, 2409 (1992).
8. E. Mattsson, and A.-M. Fredriksson, *Br. Corros. J.*, **3**, 246 (1968).
9. M. Drogowska, L. Brossard, and H. Menard, *J. Electrochem. Soc.*, **139**, 39 (1992).
10. J.-P. Duthil, G. Mankowski, and A. Giusti, *Corros. Sci.*, **38**, 1839 (1996).
11. M. Pourbaix, *Atlas of Electrochemical Equilibria in Aqueous Solutions*, p. 599, NACE International Cebelcor, (1974).
12. M.B. Ives, Y.C. Lu, and J.L. Luo, *Corros. Sci.*, **32**, 91 (1991).
13. N.D. Budiansky, F. Bocher, H. Cong, M.F. Hurley, and J.R. Scully, in, *Proceedings of NACE-Corrosion 2006*, San Diego, CA, USA, (2006)
14. A.J. Sedriks, *Corrosion of Stainless Steels*, p. 1, John Wiley & Sons, Inc., New York, (1996).
15. H.S. Campbell, *J. Inst. Met.*, **77**, 345 (1950).

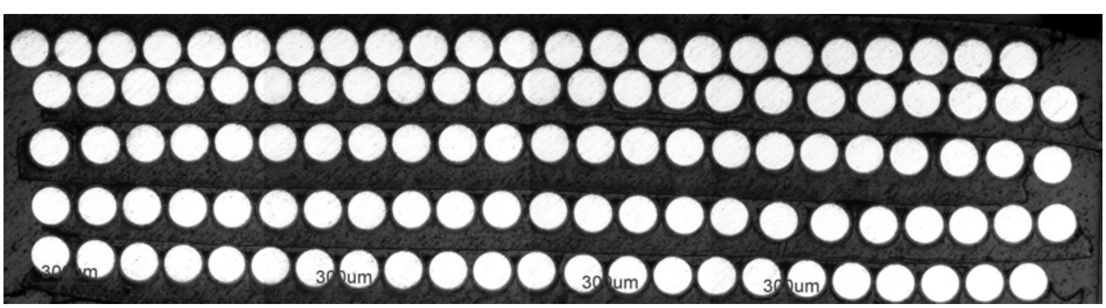

FIGURE 1. Cross section of a 5x20 multi-electrode array made from one hundred 150 µm diameter single Cu wires (Area of rectangle is 2.25 mm^2).

Downloaded on 2016-09-15 to IP 130.203.136.75 address. Redistribution subject to ECS terms of use (see ecsdl.org/site/terms_use) unless CC License in place (see abstract).

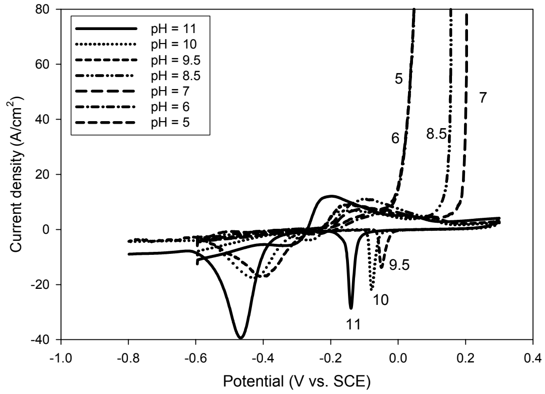

FIGURE 2. E vs. i behavior from cyclic voltammetry on a 250 μm diameter Cu wire in different pH synthetic water at 25 ºC. Passivation of the copper surface breaks down at pH ≤ 8.5.

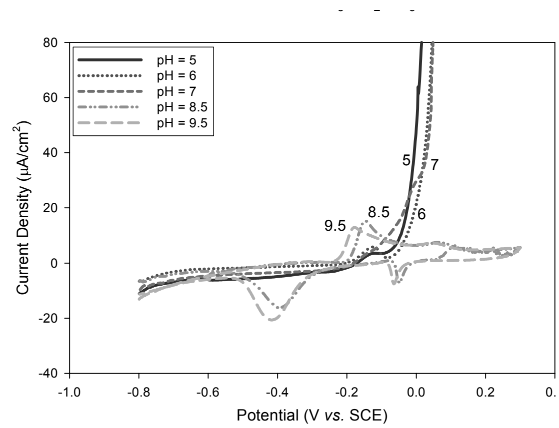

FIGURE 3. E vs. i behavior from cyclic voltammetry on a 250 μm diameter Cu wire in 0.01 M $H_2CO_3/HCO_3^-/CO_3^{2-}$ solutions at different pHs at 25 ºC.

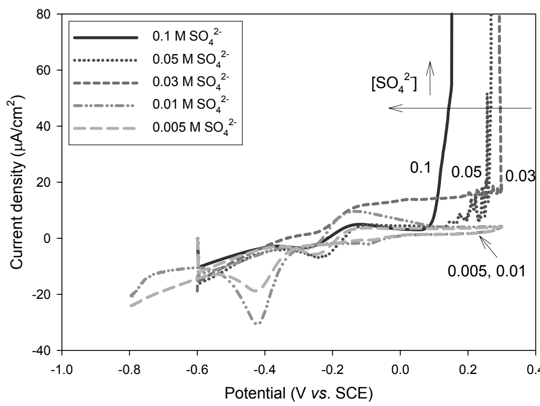

FIGURE 4. E vs. i behavior from cyclic voltammetry on a 250 μm diameter copper wire in pH = 8.3, 0.01 M HCO_3^- based solution with the [SO_4^{2-}] varied from 0.005 M to 0.1 M in individual tests at 25 ºC. Stable pitting occurred when [SO_4^{2-}] ≥ 0.03 M.

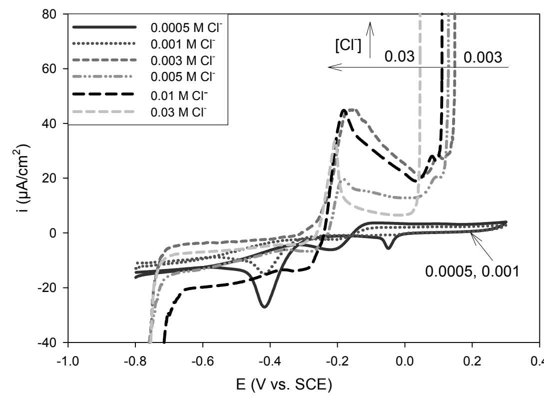

FIGURE 5. E vs. i behavior from cyclic voltammetry on a 250 μm diameter copper wire in pH = 9.5, 0.001 M HCO_3^- based solution with [Cl^-] varied from 0.0005 M to 0.03 M. Pitting stabilization occurred when [Cl^-] ≥ 0.003 M.

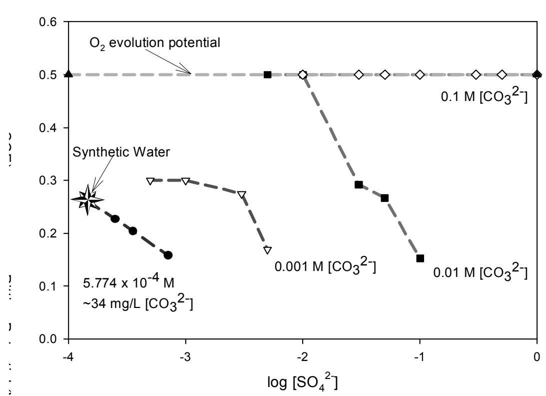

FIGURE 6. E—SO_4^{2-}—HCO_3^- pitting stability domain at pH = 8.3.

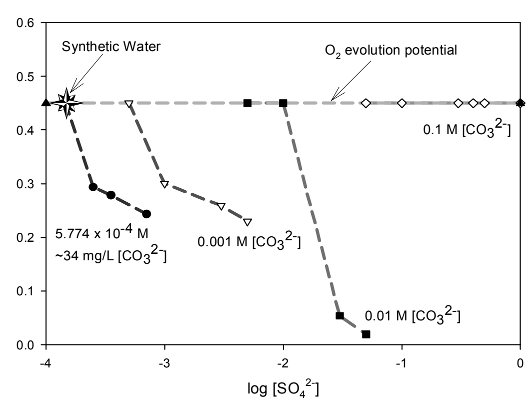

FIGURE 7. E—SO_4^{2-}—HCO_3^- pitting stability domain at pH = 9.5.

Downloaded on 2016-09-15 to IP 130.203.136.75 address. Redistribution subject to ECS terms of use (see ecsdl.org/site/terms_use) unless CC License in place (see abstract).

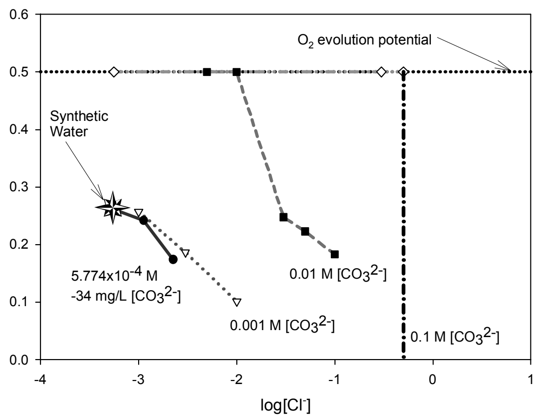

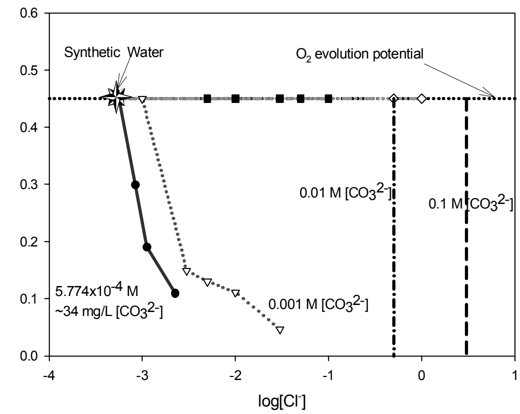

FIGURE 8. E—Cl-—HCO3- pitting stability domain at pH = 8.3.

FIGURE 9. E—Cl^-—HCO_3^- pitting stability domain at pH = 9.5.

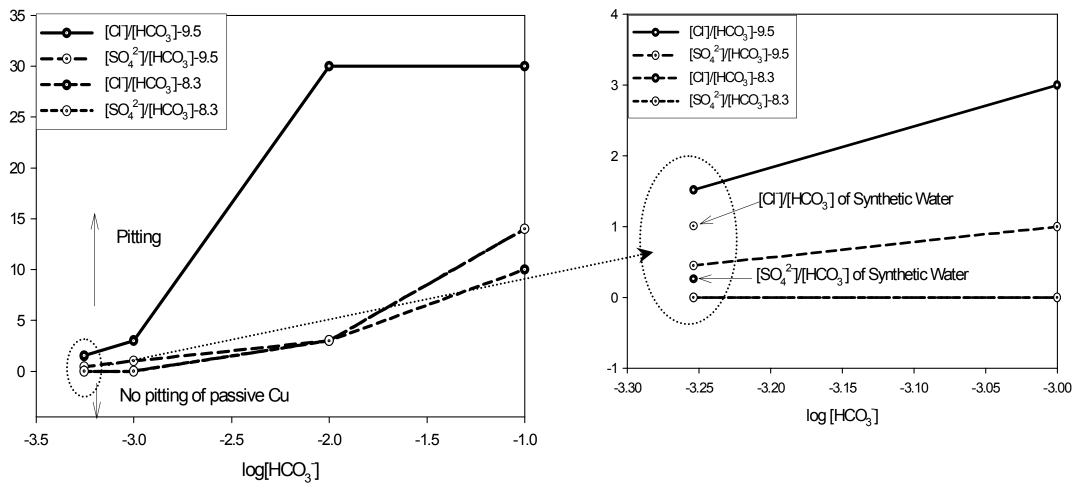

FIGURE 10. Critical ion ratio that causes pitting for various $[Cl^-]/[HCO_3^-]$ and $[SO_4^{2-}]/[HCO_3^-]$ ratios at pH = 8.3 and pH = 9.5 at 25 ºC.

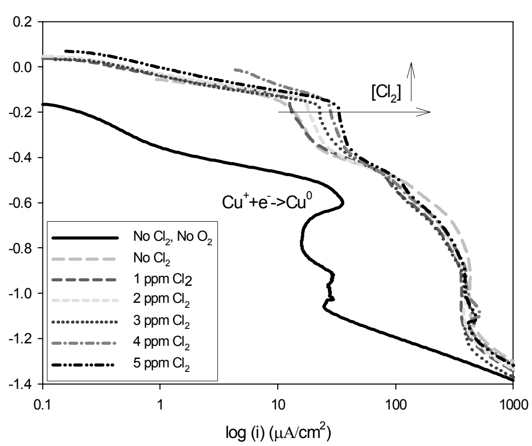

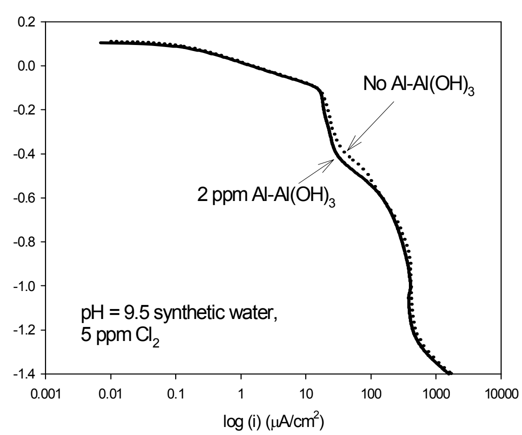

FIGURE 11. E vs. i behavior from a cathodic polarization scan on a 150 μm diameter Cu wire in pH = 9.5 synthetic water at 25 ºC. Water was deaerated or aerated as indicated, and free chlorine concentration was varied from 1 ppm to 5 ppm.

FIGURE 12. E vs. i behavior from a cathodic polarization scan on a 150 μm diameter copper wire in pH = 9.5, 5 ppm free Cl_2 synthetic water at 25 ºC. 2 ppm Al-$Al(OH)_3$ was added to study the effect of Al solids in the cathodic process.

Downloaded on 2016-09-15 to IP 130.203.136.75 address. Redistribution subject to ECS terms of use (see ecsdl.org/site/terms_use) unless CC License in place (see abstract).

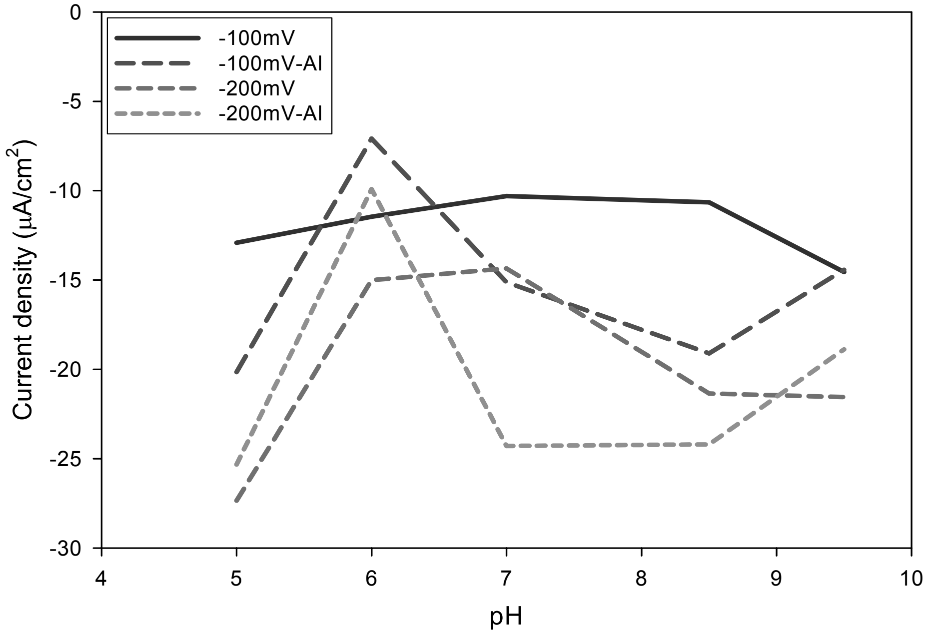

FIGURE 13. Current densities extracted from cathodic polarization curves at E = -0.1 V and E = -0.2 V in 5 ppm Cl2 synthetic water at room temperature. pH varied from 5 to 9.5.

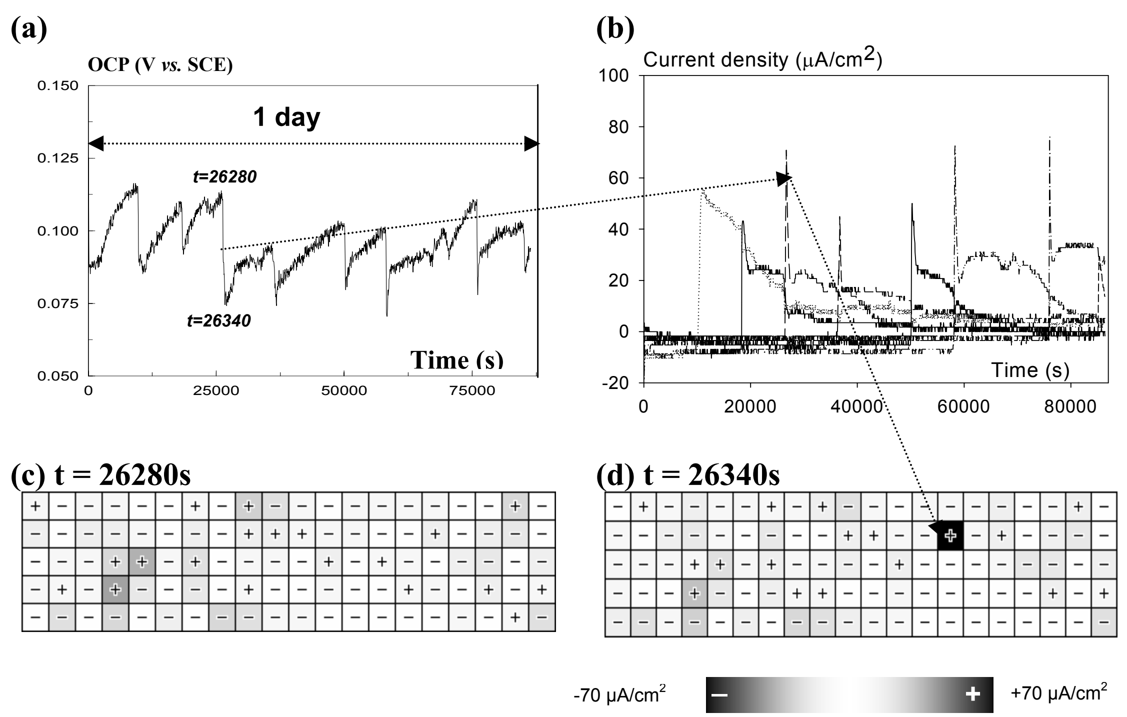

FIGURE 14. (a) OCP vs. time and (b) local current density vs. time for 8 Cu wires that formed pits after 5 ppm free chlorine was added in pH = 9 synthetic drinking water with 2 ppm Al. Stationary current maps at time t = 26,280 s (c) and t = 26340 s (d). One electrode begins pitting actively, as shown by the dark color with a plus sign, indicating a high anodic dissolution rate.

Downloaded on 2016-09-15 to IP 130.203.136.75 address. Redistribution subject to ECS terms of use (see ecsdl.org/site/terms_use) unless CC License in place (see abstract).

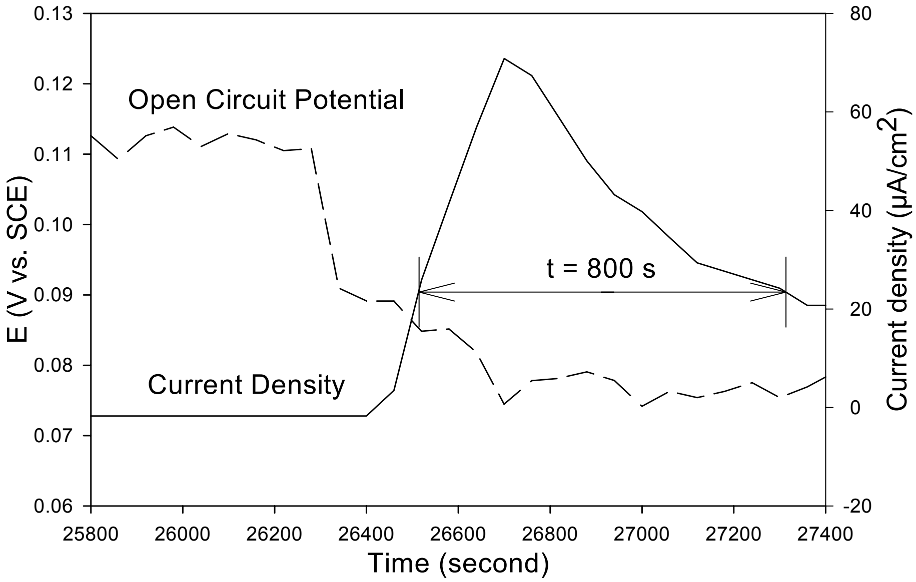

FIGURE 15. Potential and current versus time behavior for the actively pitted wire shown in FIGURE 14 (d) indicated by the dark black square. The initiation and propagation of pitting on the single wire lasted about 15 minutes.

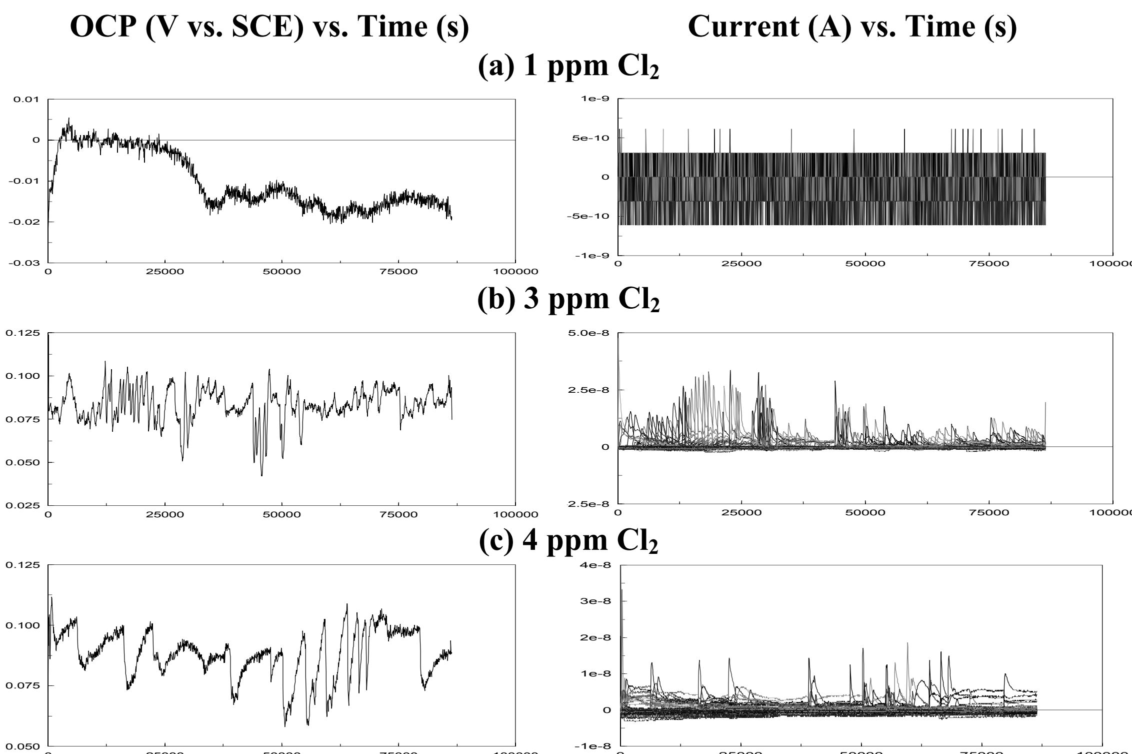

FIGURE 16. Potential-time series and corresponding current-time series for all 100 wires for MEA experiments in pH = 9 synthetic water with 2 ppm Al-Al$(OH)_3$ in addition to (a) 1 ppm Cl_2, (b) 3 ppm Cl_2, and (c) 4 ppm Cl_2.

Downloaded on 2016-09-15 to IP 130.203.136.75 address. Redistribution subject to ECS terms of use (see ecsdl.org/site/terms_use) unless CC License in place (see abstract).